Proceedings of the 12th International and 52nd National Conference on Fluid Mechanics and Fluid Power (FMFP)
December 19-21, 2025, Nirma University, Gujarat, India

FMFP2025-FSF-065

Memory-Driven Diffusion in Fluids

Atharva D. Joshi[1] and Gaurav Bhutani[2,*]

[1] Department of Mathematics, Indian Institute of Science Education and Research (IISER) Bhopal,Madhya Predesh 462066, India
[2]School of Mechanical and Materials Engineering, Indian Institute of Technology (IIT) Mandi, Himachal Pradesh 175075, India

Emails: atharvajoshi23@iiserb.ac.in; gaurav@iitmandi.ac.in

ABSTRACT

Classical diffusion is described by Gaussian behavior, where the mean squared displacement (MSD) of particles grows linearly with time. However, fluid transport in many complex systems—such as turbulent flows, porous media, and viscoelastic suspensions—often deviates from this classical picture, exhibiting anomalous diffusion. Such anomalous diffusion can be either slower (subdiffusion) or faster (superdiffusion) compared to classical predictions. In subdiffusive scenarios, particle movements depend strongly on the past states of the system, indicating significant memory effects. Fractional calculus provides a natural framework to capture these memory-driven processes by introducing fractional derivatives, which inherently incorporate historical information through a memory kernel. In this work, we study the one-dimensional time-fractional diffusion equation, where the fractional order α directly represents the memory strength of the medium. Although fractional models are powerful, their widespread application has been limited by the scarcity of reliable analytical benchmarks for code validation. Here, we derive an explicit Green-function solution to the one-dimensional fractional diffusion equation. Our approach employs a numerically stable integral representation of the Mittag–Leffler function. The derived solution clearly shows how reducing the fractional order α enhances subdiffusive behavior, and smoothly recovers the classical Gaussian kernel when α approaches unity. This robust analytical benchmark will enable researchers to confidently validate and advance numerical methods for modeling memory-driven transport in complex fluid systems.
Keywords: fractional diffusion; fractional differential equations; subdiffusion; Mittag–Leffler function; analytical solution

I. INTRODUCTION

Diffusion is fundamental in transporting heat, momentum, and chemical species in liquids, gases, and complex suspensions. Traditionally, diffusion is described by Gaussian statistics, where a localized disturbance spreads out at a rate proportional to the square root of time. However, numerous experiments, particularly tracer tests in fractured geological media [2], demonstrate that substances often spread significantly slower than classical diffusion predicts. Such slower-than-expected spreading is known as subdiffusion, and arises from the medium's capacity to "remember" past particle states, causing long-lasting influences on transport behavior.

Fractional calculus, which generalizes traditional calculus to non-integer derivatives, has emerged as a powerful mathematical approach to capture these memory effects. By substituting classical derivatives with fractional Caputo derivatives, fractional diffusion equations naturally incorporate history-dependent transport [4], [6]. These fractional models have proven broadly applicable, describing phenomena such as scalar mixing in turbulent flows [5], anomalous dispersion in groundwater systems [1], and flow in viscoelastic channels [8].

Despite their versatility, fractional diffusion models face two significant practical challenges. Firstly, researchers typically rely on numerical approaches due to a lack of robust analytical solutions, limiting the ability to verify computational codes and benchmark new methods. Secondly, fractional models involve the Mittag–Leffler function, which is numerically unstable when evaluated using standard series expansions on the negative real axis, complicating its practical computation.

To overcome these challenges, this paper revisits the one-dimensional fractional diffusion equation with a Caputo fractional derivative. We specifically consider an initial Dirac-delta pulse, representative of a point-source release scenario. By applying joint Fourier and Laplace transforms, we derive a fractional Green function expressed through an integral involving the Mittag–Leffler function. We then evaluate this integral using a numerically stable real-axis integral representation nested inside a cosine integral, utilizing adaptive numerical quadrature. Integration limits are carefully selected such that numerical errors remain negligible (below 10^{-6}), thus achieving double-precision accuracy.

The paper is organized as follows: Section II describes the methodology, outlining the analytical derivation of the fractional Green function and explaining the numerical techniques used for its evaluation. Section III presents and discusses the numerical analysis of the analytical solution, highlighting how the fractional order α impacts the spectral characteristics of the kernel, the Green-function integrand behavior, and the resulting spatial and temporal concentration profiles. Finally, Section IV summarizes the key findings, emphasizing the utility of our Green-function solution as an analytical benchmark, and suggests directions for future research involving numerical methods for memory-driven diffusion processes in fluid mechanics.

II. METHODOLOGY

A. Analytical formulation

We consider the one-dimensional time-fractional diffusion equation involving a Caputo fractional derivative of order $0 < \alpha \leq 1$:

$$\frac{\partial^\alpha u(x,t)}{\partial t^\alpha} = D^2 \frac{\partial^2 u(x,t)}{\partial x^2}, \tag{1}$$

where $u(x,t)$ is the scalar field representing concentration, temperature, or a similar transport property, x is the spatial coordinate, t denotes time, α indicates the fractional order, and D^2 is the generalized diffusion coefficient.

The initial condition is taken as an instantaneous point-source located at position x_0, mathematically expressed as:

$$u(x,0) = c\,\delta(x - x_0), \tag{2}$$

where c is the source magnitude, and $\delta(\cdot)$ denotes the Dirac delta function. To complete the formulation, we impose the boundary condition that the solution must vanish at infinity:

$$\lim_{|x|\to\infty} u(x,t) = 0 \quad (t > 0). \tag{3}$$

The Caputo fractional derivative used here is defined as:

$$\frac{\partial^\alpha f(t)}{\partial t^\alpha} = \frac{1}{\Gamma(n-\alpha)} \int_0^t (t-\tau)^{n-\alpha-1} \frac{d^n f(\tau)}{d\tau^n}\, d\tau, \quad n-1 < \alpha < n, \tag{4}$$

where n is the smallest integer greater than α, and $\Gamma(\cdot)$ is the Gamma function.

We derive the analytical solution by first applying a spatial Fourier transform followed by a temporal Laplace transform. This approach simplifies the fractional partial differential equation into an algebraic equation. Inverting these transforms then provides the fractional Green function solution expressed as:

$$u(x,t) = c\,G(x - x_0, t), \tag{5}$$

where the Green function $G(x,t)$ is given by the integral:

$$G(x,t) = \frac{1}{\pi} \int_0^\infty E_{\alpha,1}\left(-D^2 k^2 t^\alpha\right) \cos(kx)\, dk. \tag{6}$$

Here, $E_{\alpha,\beta}(z)$ denotes the two-parameter Mittag–Leffler function, defined by:

$$E_{\alpha,\beta}(z) = \sum_{m=0}^{\infty} \frac{z^m}{\Gamma(\alpha m + \beta)}. \tag{7}$$

In the special case $\alpha = 1$, the Mittag–Leffler function reduces to an exponential, $E_{1,1}(z) = e^z$, and thus the fractional Green function simplifies to the classical Gaussian kernel:

$$G_{\text{Gaussian}}(x,t) = \frac{1}{\sqrt{4\pi D^2 t}} \exp\left(-\frac{x^2}{4D^2 t}\right). \tag{8}$$

B. Numerical evaluation of the Green's function

The integral form of the Green function $G(x,t)$ derived above does not possess a simple closed-form solution and thus must be evaluated numerically. The numerical computation involves two main steps: first, ensuring a stable evaluation of the Mittag–Leffler kernel; second, accurately integrating the resulting Green-function integral.

For negative arguments and fractional orders $0 < \alpha < 1$, the direct series expansion of the Mittag–Leffler function is numerically unstable. To avoid this instability, we employ a robust integral representation along the real axis:

$$E_{\alpha,1}(z) = -\frac{z \sin(\pi\alpha)}{\pi\alpha} \int_0^\infty \frac{e^{-r^{1/\alpha}}}{r^2 - 2rz\cos(\pi\alpha) + z^2}\, dr, \quad z < 0, \tag{9}$$

as proposed by Gorenflo, Loutchko and Luchko [3]. We evaluate this integral numerically using adaptive Gauss–Kronrod quadrature for each wavenumber k in the Green function integral. Because the prefactor contains $\sin(\pi\alpha)$, this representation is not strictly valid at $\alpha = 1$; hence, we approximate the Gaussian limit numerically using a fractional order $\alpha = 0.99$.

The outer integral for $G(x,t)$ is numerically evaluated up to an adaptive upper limit UL, chosen such that the magnitude of the integrand becomes negligible, i.e. $|E_{\alpha,1}(-D^2k^2t^\alpha)| < 10^{-6}$, beyond this point. Both inner (Mittag–Leffler kernel) and outer (Green function integral) integrations are performed using adaptive Gauss–Kronrod quadrature on uniformly spaced grids for fractional orders $\alpha \in [0.5, 0.99]$.

III. RESULTS AND DISCUSSION

A. Mittag–Leffler kernel in k-space

Figure 1 shows the decay behavior of the Mittag–Leffler kernel $E_{\alpha,1}\left(-D^2k^2t^\alpha\right)$ as a function of wavenumber k for different fractional orders α. In the classical diffusion limit ($\alpha = 1$), the kernel decays rapidly and exponentially, implying quick suppression of higher spatial-frequency modes. As the fractional order decreases from 0.99 down to 0.5, this decay becomes progressively slower, resulting in heavier tails in the k-space.

From a physical perspective in fluid mechanics, these heavy tails indicate enhanced memory effects within the fluid medium. In the integral solution for the concentration, each spatial frequency contributes according to this kernel. Therefore, lower fractional orders keep significant contributions from higher wavenumbers for longer durations. Practically, this means that sharp concentration gradients formed by a localized source persist much longer compared to the classical diffusion case, consistent with observations in subdiffusive systems such as fractured rocks and viscoelastic suspensions [2], [5].

The kernel values are computed numerically using the stable integral formulation provided by Gorenflo et al. [3], ensuring numerical stability for fractional orders $0 < \alpha < 1$.

B. Green-function integrand

Figure 2 illustrates the integrand $f(k) = t^{\alpha-1} E_{\alpha,1}\left(-D^2k^2t^\alpha\right)\cos(kx)$ for two fractional orders:

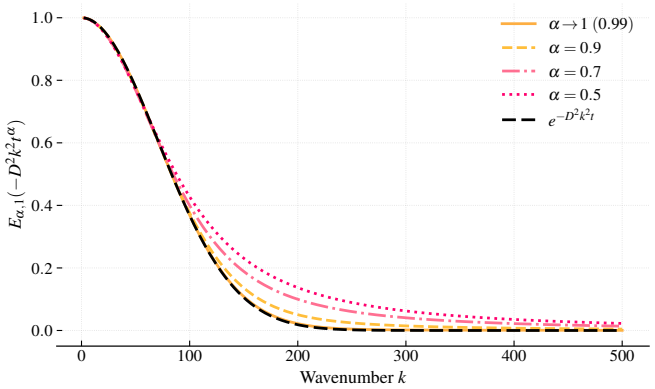

Figure 1: **Decay of Mittag–Leffler kernel** $E_{\alpha,1}(-D^2k^2t^\alpha)$ **in wavenumber space for fractional orders** $\alpha = 0.5, 0.7, 0.9, 0.99$**. The classical exponential decay corresponding to standard diffusion** ($\alpha = 1$) **is shown as dashed. Parameters:** $D = 0.01$**,** $t = 1$**. Smaller fractional orders lead to slower decay, indicative of stronger memory and longer persistence of initial spatial structures. Kernel evaluated using stable integral method [3].**

near-classical diffusion ($\alpha = 0.99$) and strong subdiffusion ($\alpha = 0.5$). The cosine term dictates the oscillatory nature, while the envelope amplitude is set by the Mittag–Leffler kernel. Due to slower kernel decay for lower fractional orders, significant contributions to the integrand persist at high wavenumbers. Consequently, to accurately compute the integral for subdiffusive transport, a broader integration range must be used to capture these persistent high-frequency modes. Physically, this ensures the memory effects and sharper gradients are correctly represented in the final concentration distribution.

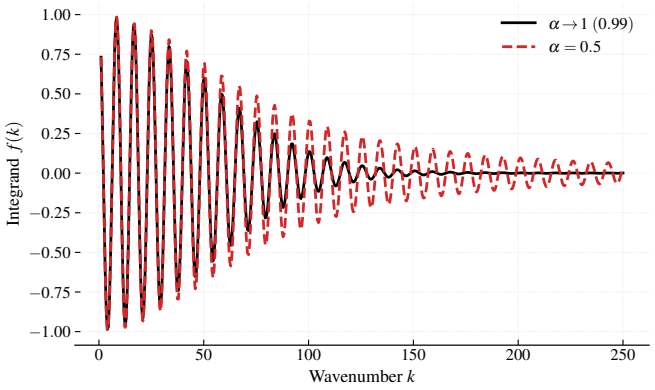

Figure 2: **Comparison of Green-function integrand for fractional orders** $\alpha = 0.99$ **(black) and** $\alpha = 0.5$ **(red) at** $t = 2$**,** $x = 0.75$**,** $D = 0.01$**. The integrand for** $\alpha = 0.5$ **shows pronounced oscillations with slower amplitude decay, indicative of prolonged spectral influence contributing to subdiffusion.**

C. Spatial Green-function profiles

Figure 3 presents spatial concentration profiles $G(x,t)$ at a fixed time $t = 2$ for various fractional orders. The classical diffusion ($\alpha = 1$) profile is broad and Gaussian-shaped (dashed curve). In contrast, as fractional order decreases from 0.99 to 0.5, the concentration profiles become progressively narrower and higher at the center. This indicates a slower and more restricted spread, clearly representing subdiffusion.

Physically, this narrowing occurs because particles in media with stronger memory do not freely diffuse away from their original position. Instead, the medium's memory reduces particle mobility, keeping the distribution sharply peaked. Such behavior aligns with experimental observations of slow tracer dispersion in complex media like fractured rocks and polymeric fluids [7], [2].

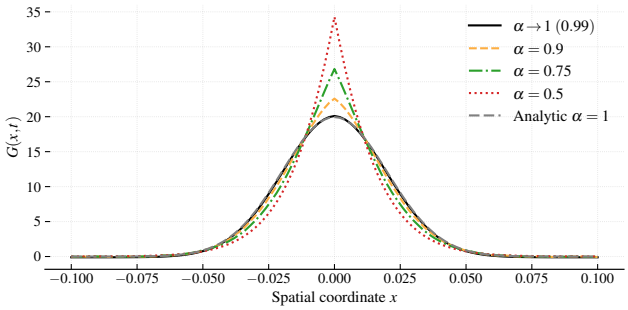

Figure 3: **Spatial profiles of Green function** $G(x,t)$ **at** $t = 2$ **for fractional orders** $\alpha = 0.5, 0.75, 0.9, 0.99$**, with classical Gaussian solution** ($\alpha = 1$) **as dashed line. Lower fractional orders yield sharper peaks and narrower profiles, indicating slower spreading and stronger memory-driven confinement.**

D. Temporal Green-function at the source

Figure 4 shows the concentration at the source location ($x = 0$) as it evolves over time for several fractional orders. Due to spatial symmetry, this also represents the maximum concentration at each instant. The classical diffusion case ($\alpha = 1$) peaks early and rapidly decreases thereafter. As the fractional order decreases, the peak concentration occurs later in time, reaches higher values, and subsequently decays more slowly. This clearly demonstrates how stronger memory significantly delays mass dispersion and retains particles close to the origin for longer periods, a hallmark of subdiffusion.

E. Temporal spread for a subdiffusive order ($\alpha = 0.8$)

Figure 5 illustrates how the concentration profile evolves spatially at successive times for a fixed fractional order ($\alpha = 0.8$). Although the peak gradually decreases and the distribution widens over time, it remains significantly narrower than the classical diffusion prediction ($\alpha = 1$). This persistent narrowness, even at later times, indicates that the medium's memory continues to strongly constrain particle spreading. The mass stays concentrated close to the origin far longer than it would under classical diffusion.

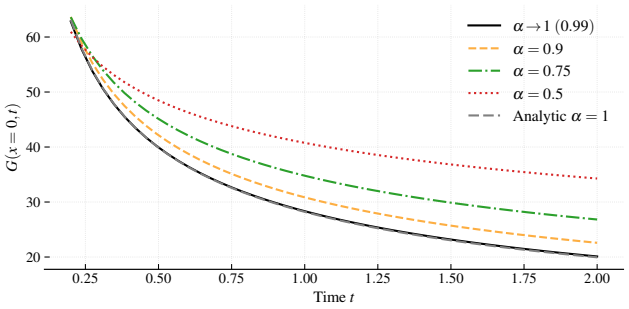

Figure 4: **Temporal evolution of concentration at the source** ($x = 0$) **for fractional orders** $\alpha = 0.5, 0.75, 0.9, 0.99$**. The dashed curve** ($\alpha = 1$) **shows the classical Gaussian diffusion. Lower fractional orders delay peak concentration and prolong decay, demonstrating memory effects that enhance retention of mass near the source.**

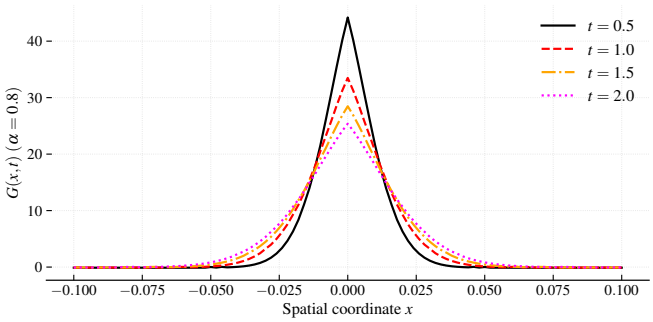

Figure 5: **Spatial concentration profiles for fractional order** $\alpha = 0.8$ **at times** $t = 0.5, 1, 1.5, 2$**. Despite gradual broadening over time, the distribution remains distinctly narrower than classical Gaussian diffusion, reflecting sustained memory effects that slow spatial dispersion. Parameters:** $D = 0.01$**.**

Collectively, these results illustrate how fractional-order diffusion models effectively capture the memory-dependent behavior observed in complex fluid systems. Comparison of the analytical solution against the traditional Gaussian case confirms the accuracy of the derived Green-function solution, reinforcing its utility as a robust benchmark for modeling subdiffusive transport phenomena relevant to diverse fluid mechanics applications.

IV. CONCLUSIONS

In this study, we derived and analyzed a stable, explicit Green-function solution for the one-dimensional time-fractional diffusion equation incorporating a Caputo fractional derivative. By utilizing a numerically stable real-axis integral representation of the Mittag–Leffler function, we successfully obtained accurate solutions over the entire fractional order range $0 < \alpha < 1$.

Numerical evaluations reveal that as the fractional order α decreases, the spectral decay of the kernel becomes slower, resulting in spatial concentration profiles that are taller and narrower compared to the classical Gaussian case. Additionally, temporal responses at fixed locations show delayed peak arrival and prolonged decay, clearly reflecting subdiffusive behavior driven by memory effects. Importantly, our derived solution consistently recovers the classical Gaussian diffusion kernel as $\alpha \to 1$, verifying both its correctness and physical relevance.

The explicit Green-function solution presented here serves as a reliable analytical benchmark, enabling researchers to validate and enhance numerical methods for fractional diffusion equations. It provides a foundation to explore more complex fractional transport phenomena relevant to fluid mechanics, such as turbulent mixing, tracer dispersion in porous media, and viscoelastic flows.

Building upon this benchmark, future studies will investigate broader classes of fractional partial differential equations and incorporate advanced solution strategies like the Method of Moments (MoM) and machine learning (ML) techniques. These approaches will be tailored to address the intricate dynamics arising from memory-dependent processes in fluid transport.

ACKNOWLEDGEMENTS

The authors gratefully acknowledge the financial support received from the Science and Engineering Research Board (SERB), Department of Science and Technology, Government of India, under the MATRICS scheme (Sanction No. MTR/2022/000894).

NOMENCLATURE

α	Fractional order of the time derivative	[-]
D^2	Generalized diffusion coefficient	$\mathrm{m}^2\,\mathrm{s}^{-\alpha}$
$u(\cdot)$	Scalar field (concentration, temperature, etc.)	[varies]
x	Spatial coordinate	m
t	Time	s
k	Wavenumber (integration variable)	m^{-1}
c	Source strength (Dirac pulse magnitude)	[varies]
$E_{\alpha,\beta}(\cdot)$	Two-parameter Mittag–Leffler function	[-]
$G(\cdot)$	Fractional Green function (solution kernel)	[varies]
$\Gamma(\cdot)$	Gamma function	[-]
$\delta(\cdot)$	Dirac delta function	[-]

REFERENCES

[1] D. A. Benson, S. W. Wheatcraft, and M. M. Meerschaert, *Application of a fractional advection–dispersion equation*, Water Resources Research **36** (2000), no. 6, 1403–1412.

[2] B. Berkowitz, A. Cortis, M. Dentz, and H. Scher, *Modeling non-Fickian transport in geological formations as a continuous time random walk*, Reviews of Geophysics **44** (2006), no. 2, RG2003.

[3] R. Gorenflo, J. Loutchko, and Y. Luchko, *Computation of the Mittag-Leffler function $E_{\alpha,\beta}(z)$ and its derivative*, Fractional Calculus and Applied Analysis **5** (2002), no. 4, 491–518.

[4] I. Podlubny, *Fractional Differential Equations*, Mathematics in Science and Engineering, vol. 198, Academic Press, San Diego, 1999.

[5] R. L. Magin and M. Ovadia, *Modeling the fractional dynamics of turbulent diffusion*, Communications in Nonlinear Science and Numerical Simulation **15** (2010), no. 4, 972–981.

[6] F. Mainardi, *Fractional Calculus and Waves in Linear Viscoelasticity*, World Scientific, Singapore, 2010.

[7] R. Metzler and J. Klafter, *The random walk's guide to anomalous diffusion: a fractional dynamics approach*, Physics Reports **339** (2000), no. 1, 1–77.

[8] M. Zayernouri and G. E. Karniadakis, *Fractional spectral collocation methods for linear and nonlinear fractional differential equations*, Journal of Computational Physics **252** (2013), 495–517.